International Council for the Exploration of the Sea

ICES CM 2006/I:13

Estimating and decomposing total uncertainty for survey-based abundance estimates of Norwegian spring-spawning herring

Magne Aldrin Anders Løland

Abstract

We demonstrate how the total uncertainty of the abundance estimate and abundance-at-age estimate of Norwegian spring-spawning herring are affected by uncertainty in the parameters of vessel avoidance, shadowing and depth dependent target strength, and uncertainty from trawl hauls and spatial-temporal coverage. The total uncertainty is decomposed into the sum of the contribution from each source separately. In addition, we highlight the potentially dramatic combined effect of correcting for vessel avoidance, shadowing and depth dependent target strength on the abundance estimate. The main framework is believed to be a promising tool for focusing the effort for reducing the uncertainty in the abundance estimates. The method is applied to data from surveys on the over-wintering stock in the Vestfjord system and Vesteraalen in northern Norway in November/December in the years 2001–2004.

Keywords: total uncertainty, uncertainty decomposition, abundance estimation

Contact author:

Magne Aldrin: Norwegian Computing Center, Gaustadalléen 23, P.O. Box 114 Blindern, NO-0314 Oslo, Norway. [Tel.: +47 22 85 25 00, Fax: +47 22 69 76 60. E-mail: magne.aldrin@nr.no.]

1 Introduction

Norwegian spring-spawning herring is the largest fish stock in the Northeast Atlantic. The herring stock spawns along the Norwegian coast, feeds in the Norwegian Sea and over-winters in the Vestfjord system and, in recent years, in Vesteraalen, outside the Vestfjord system. Since 2003, the majority of the stock has over-wintered in Vesteraalen.

The Institute of Marine Research (IMR) surveys the stock on a regular basis to get estimates of age-specific abundance, which are of vital importance for the assessment and management of the stock. The winter survey is carried out in the Vestfjord system and Vesteraalen in November/December each year. Here, the spatial density of fish is measured with acoustics and age/length data are gathered from trawling. These data are combined into abundance-at-age.

The standard total abundance estimate (Thoresen et al., 1998) is based on the assumption that the acoustic signal is proportional to the number of fish and the average squared length of fish. Abundance-at-age is further found by using the observed age proportions. However, this may give serious bias due to the shadowing effect (Zhao and Ona, 2003), depth dependent target strength (Ona, 2003) and vessel avoidance (Vabø et al., 2002). IMR has already for some years used an improved estimator correcting for the shadow effect. Further improvements that accounts for depth dependent target strength and vessel avoidance as well is under development, and will be adopted within a few years. Here we present a preliminary version of the new improved estimator.

Traditionally, the uncertainty of the abundance estimates has either not been quantified at all, or only a part of the uncertainty has been quantified, even though it is increasingly recognised that uncertainty should be taken into account in the management of a fish stock. The main focus of this paper is to present a method to quantify the uncertainties of the total and age-specific abundance estimates, taking into account the combined effect of several sources of uncertainty. Furthermore, we show how the total uncertainty may be decomposed into the sum of the contribution from each source separately. Such a decomposition may be used to identify the most important contributors to the total uncertainty and suggests where one should put the effort to make future surveys more cost-effective.

We have identified five important sources to the total uncertainty. These are uncertainty due to age/length from trawling, spatial-temporal uncertainty due to incomplete coverage in space and time and the three acoustic signal corrections mentioned above. First, the uncertainty is quantified for each source separately. The spatial-temporal and the age/length uncertainties are estimated and represented by non-parametric bootstrap. The acoustic signal corrections are described by parametric functions, where the form of the functions are assumed to be error-free, but whose parameters are uncertain with a quantified uncertainty (Foote, 1999; Ona, 2003). The uncertainty of these sources are represented by simulating parameter values from the estimated distributions. Finally, the total uncertainty is found by combining the non-parametric and parametric simulations for each source, resulting in simulated values of the total and age-specific abundance estimates.

This paper is organised as follows. Section 2 presents the data, from the November/December surveys from 2001–2004. Section 3 describes the abundance estimation procedure, the three correction methods and how the total uncertainty is computed and decomposed. The results of our study are given in Section 4. Some concluding remarks are given in Section 5.

2 Data

The data consist of acoustics and age/length data from the Norwegian spring-spawning herring November/December surveys 2001–2004. An overview of the surveys is given in Table 1. In 2001 and 2002, only the Vestfjord system was surveyed, since it was assumed that almost all of the stock over-wintered in the Vestfjord system. However, in 2002 commercial fish vessels observed young herring in the Vesteraalen area (see Figure 1), and the analysis performed in Section 4 indicates that some herring may have been in Vesteraalen already in 2002. In 2003 an equal effort was put on the Vestfjord system and in Vesteraalen. In 2004, most of the effort was put on covering Vesteraalen, since it was known that most of the fish was outside the Vestfjord system.

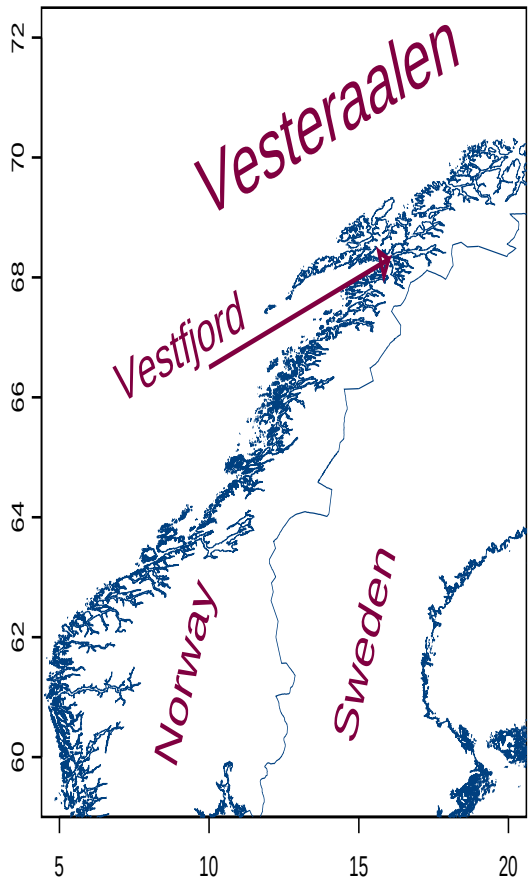

Figure 1: Map of Norway and the survey areas (the Vestfjord system and Vesteraalen).

The principal acoustic signal is the area-backscattering coefficient s_A (m^2/Nm^2). The raw signal is measured in 10 m thick depth channels averaged over 0.1 nmi (185.2 m) along the survey transects, except for the Vestfjord system 2002 and Vesteraalen 2004, where data is available on a 1 nmi scale only. For each measurement, the position $\boldsymbol{x}$ and time t is also recorded. Figure 2 shows, for the 2004 survey in both areas, the vessel transect displayed

Area and year	Date	Number of trawl stations	Number of measurements with age and length	Number of measurements with length and non-readable age	Number of measurements with length only
Vestfjord system 2001	21–29 November	9	818	81	0
Vestfjord system 2002	30 November–3 December	10	907	94	0
Vestfjord system 2003	30 November–4 December	13	1170	130	0
Vesteraalen 2003	8–18 December	10	781	219	0
Vestfjord system 2004	2–3 December	9	793	107	900
Vesteraalen 2004	5–18 December	7	677	23	601

Table 1: Survey overview, 2001–2004.

as a grey line, and the acoustic signal as circles, where the diameter is proportional to the logarithm of the signal. The signal is here integrated over the water column and averaged over 1 nmi. A large portion of the measurements are equal to zero. This can be seen where there is a survey line, but no circles.

Usually, 100 fish are chosen randomly from each haul, and the lengths (and the weights) are measured. The ages are measured from the fish scales if possible, but for approximately 10% of the fish the ages are unobservable due to worn out scales at old fish. These ages are missing non-randomly. For some trawl hauls, lengths are measured on additionally 100 fish. The ages for these fishes are not read, and are missing completely at random. Table 1 shows the number of trawl hauls for each survey. The locations where trawl sampling was performed are marked by filled triangles in Figure 2.

The data for all trawl stations from the 2004 survey are displayed in Figure 3. In Vesteraalen, there are hardly any fish older than 6 years, whereas the Vestfjord systems contains both old and young fish, but virtually none 2 years old. There are large heterogeneities between trawl hauls, i.e. one haul may consist of young fish (for instance station 3 in Vesteraalen), and another of older fish (station 7 in Vesteraalen).

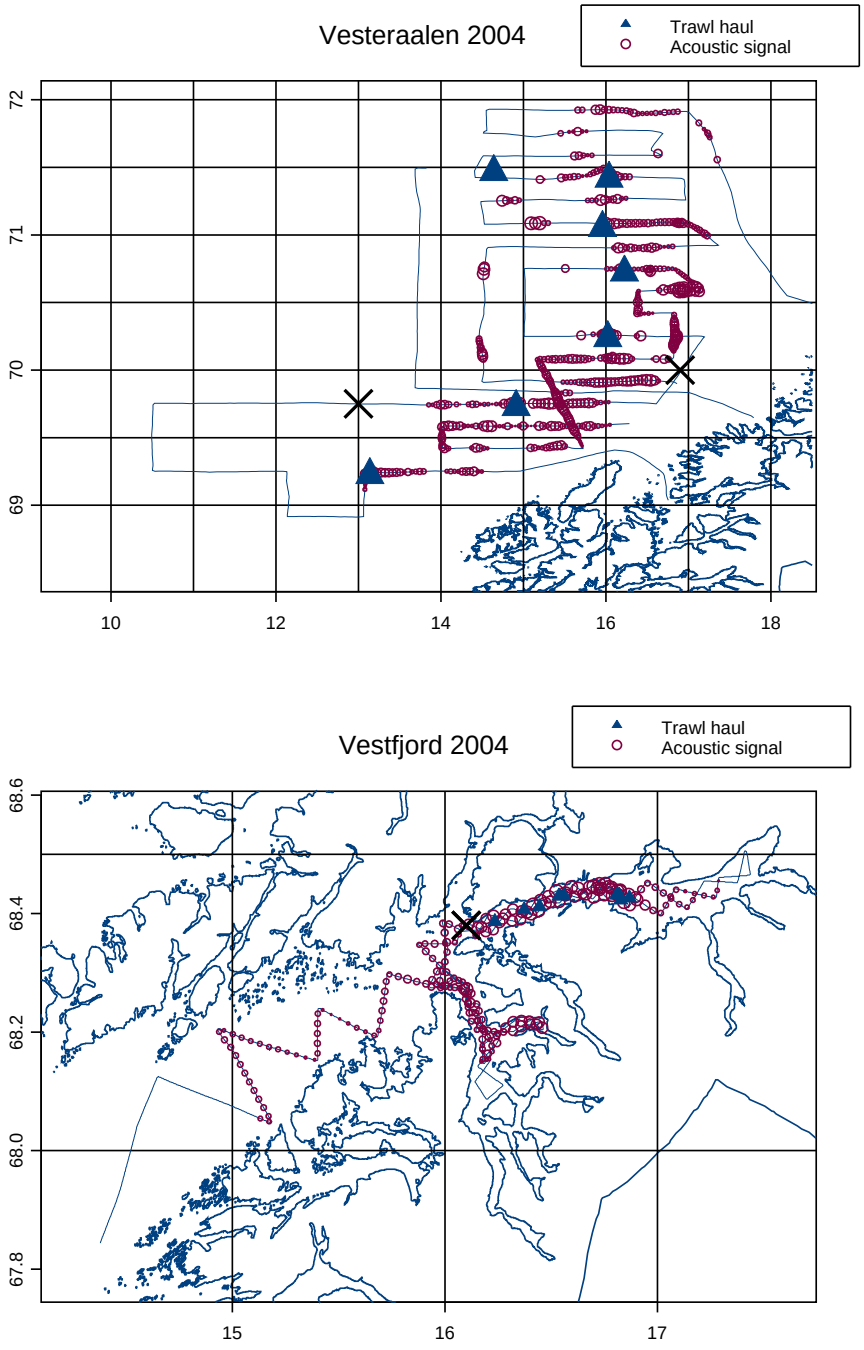

Figure 2: Overview of the surveys in the Vestfjord system 2004 and Vesteraalen 2004. The grey line represents the survey line. The red circles have diameter proportional to the acoustic signal $\log(s_A)$. No circle corresponds with a zero measurement.

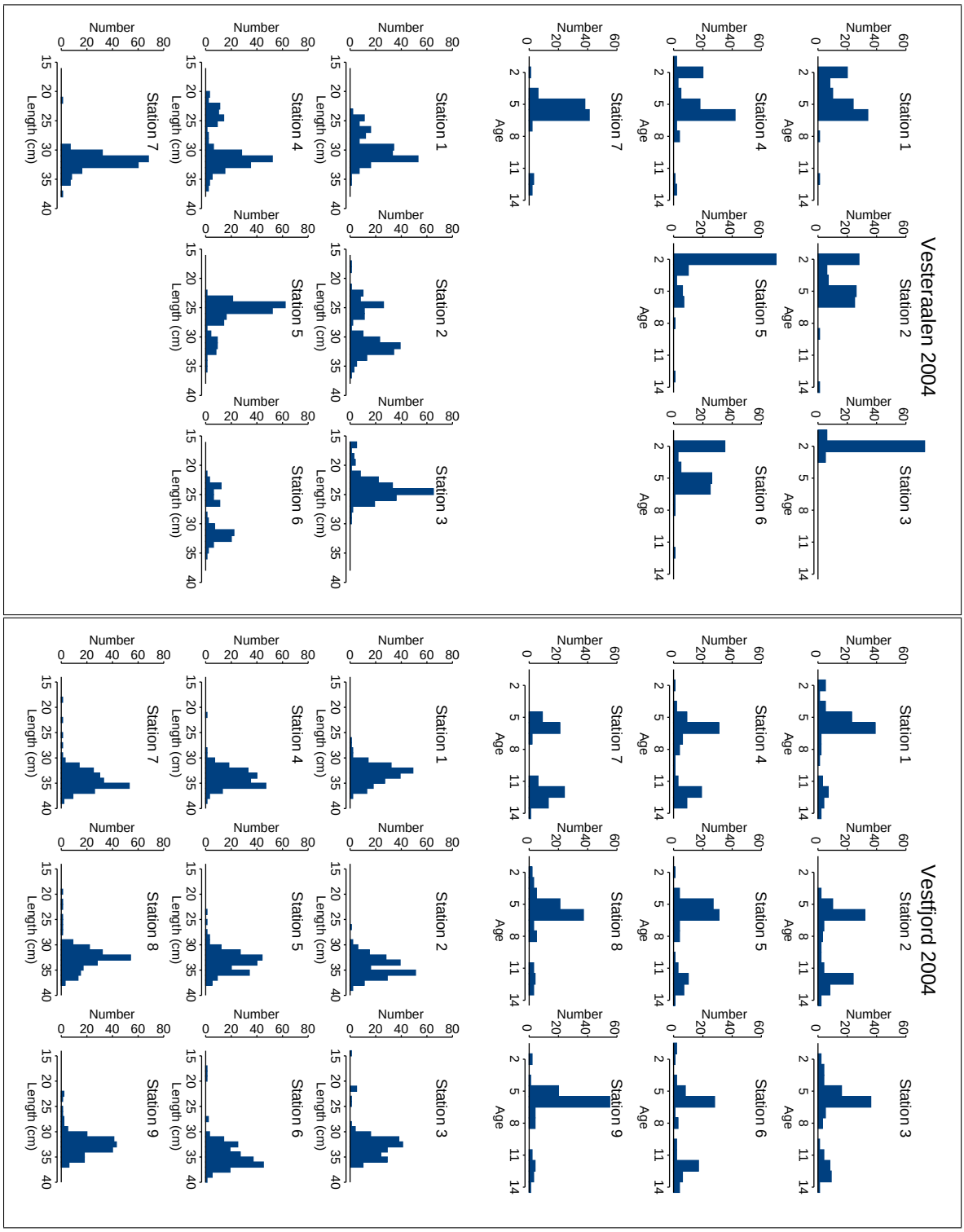

Figure 3: Histograms of age and length in the trawl hauls from the 2004 survey.

3 Method

3.1 The standard estimator

Let ρ be the average density of fish per area unit over an area of size A. The total number of fish in the area is then

$$N = \rho \cdot A. \tag{1}$$

Let further p_a be the true proportion of fish at age a. Then the number of fish at age a is given by

$$N_a = N \cdot p_a. \tag{2}$$

The standard estimates of N and N_a as defined by Thoresen et al. (1998) and Rivoirard et al. (2000) are based on the n acoustic signal measurements s_{Ai}, $i = 1, \ldots, n$, from various locations (and times) along the transects, integrated over the water column. The standard target strength (TS) relationship for herring (Foote, 1987),

$$TS = 20 \log l - 71.9\text{dB}, \tag{3}$$

gives the reflected acoustic signal from *one* fish of length l as

$$\sigma(l) = 8.1135 \cdot 10^{-7} \cdot l^2. \tag{4}$$

The fish density in location i can be estimated by

$$\hat{\rho}_i^{standard} = \frac{s_{Ai}}{\hat{\sigma}} = \frac{s_{Ai}}{8.1135 \cdot 10^{-7} \cdot \overline{l^2}}, \tag{5}$$

where $\overline{l^2}$ is the sample mean of the squared lengths of the fish in all relevant trawl hauls. This leads to the standard estimate of total abundance

$$\hat{N} = \bar{\rho} \cdot A, \tag{6}$$

where $\bar{\rho} = 1/n \sum_i \hat{\rho}_i^{standard}$ is the sample mean of the estimated densities.

Since several age measurements are missing non-randomly, the true proportion at age p_a can not be estimated (without bias) by the sample mean of the fish ages. Instead, it is estimated by

$$\hat{p}_a = \sum_l \hat{p}_{a|l} \cdot \hat{p}_l, \tag{7}$$

where $\hat{p}_l$ is the sample proportion at length group l and $\hat{p}_{a|l}$ is the sample proportion at age a, given length group l. Each length group is 1/2 cm wide. The abundance-at-age is then estimated by

$$\hat{N}_a = \hat{N} \cdot \hat{p}_a. \tag{8}$$

This procedure is performed per sub-area A, and summing over the sub-areas gives the estimates for the total area. In the Vestfjord system, the sub-areas are three separate smaller fjords (outer Vestfjord, Ofotfjord and Tysfjord). In Vesteraalen (see Figure 2), the sub-areas are squares of 1° latitude width and $1/2^\circ$ longitude height.

3.2 Improved estimator

We will now describe an improved estimator, which corrects for vessel avoidance and shadowing and incorporates an improved target strength relationship for turning the (corrected) signal into abundance of fish. The shadow correction has in fact been used for some years, and the other improvements will be adopted within a few years. The three correction factors are based on parametric functions, with parameters estimated from experimental data.

1. **Vessel avoidance:** The presence of a vessel may influence the behaviour of fish. Vabø et al. (2002) investigate the effect of vessel avoidance of wintering Norwegian spring-spawning herring and interpret the systematic changes in acoustic densities around the passing as avoidance reactions, probably due to body tilting and horizontal swimming. The effect is particularly strong down to 100 m depth. Based on the data collected by Vabø et al. (2002), we quantifie how the raw signal at passing at depth d, s_A^d, can be adjusted to the undisturbed signal before passing, $\tilde{s}_A^d$:

$$\tilde{s}_A^d = c_d (s_A^d)^b, \tag{9}$$

   where c_d and b are parameters. The correction depends both on depth and signal strength, i.e. on the density of fish.

2. **Shadowing effect:** In fish schools, there is an acoustic shadowing of fish low down in a school by those above them. The shadowing is stronger the denser the school is. The signal corrected for vessel avoidance, $\tilde{s}_A^d$, is corrected for the acoustic shadowing (first-order scattering) effect by the formula developed by Zhao and Ona (2003):

$$\tilde{\tilde{s}}_A^d = \frac{1}{K \cdot \lambda} \ln \left(\frac{1 - K \cdot \lambda \cdot \tilde{s}_A^{1:(d-1)}}{1 - K \cdot \lambda \cdot \tilde{s}_A^{1:d}} \right), \tag{10}$$

   where $\tilde{s}_A^{1:(d-1)}$ denotes the cumulative apparent area-backscattering coefficient of the fish above depth layer d and $\tilde{s}_A^{1:d}$ denotes the same from the first down to, and including, depth layer d. λ is a parameter and $K = 2/1852^2$.

3. **Depth dependent target strength – from signal to stock abundance:**

   Based on new experiments, Ona (2003) found a new target strength relationship for herring, where the target strength is depth dependent and the resulting estimated abundance is significantly lower than with the standard target strength relationship of Foote (1987). The acoustic signal reflected from *one* fish of length l at depth d is given by

$$\sigma_d(l) = 4\pi\sigma_0 \left(1 + \frac{d}{10}\right)^\gamma \frac{32^2}{10^4} l^2, \tag{11}$$

   where σ_0 and γ are parameters.

Based on the correction formulas above, the fish density in location i and depth d can be estimated by

$$\hat{\rho}_i^d = \frac{\tilde{\tilde{s}}_{Ai}^d}{4\pi \cdot \sigma_0 \cdot (1 + d/10)^\gamma \cdot 32^2/10^4 \cdot \overline{l^2}}, \tag{12}$$

and summing over all depths gives the improved estimate of the density in location i by

$$\hat{\rho}_i = \sum_d \hat{\rho}_i^d, \tag{13}$$

which replaces the estimate in Equation (5). The abundance estimates are then given by Equations (6) and (8) as before.

For each set of parameters, c_d and b (vessel avoidance), λ (shadowing) and γ and σ_0 (target strength), the parameters have been estimated with uncertainty by regression on experimental data separate for each correction, i.e. independent of each other and of the survey data.

In this paper, we have corrected for vessel avoidance before correcting for shadowing, since the parameters in Equation (9) were estimated on data without shadowing correction. It may be more natural to correct for shadowing first, but then the parameters in Equation (9) should be estimated on shadow-corrected data.

3.3 Measures of total uncertainty

The estimates of N and N_a are uncertain. We focus on estimating the standard deviations of the estimates, and use uncertainty as a synonym for standard deviation or variance here. The aim of introducing the correction factors are to minimise the bias, but we will not investigate if there still is some bias left after the correction.

We are interested in the uncertainty measures defined below. The standard deviation of the abundance estimate is denoted

$$\sigma_{\text{total}} = \mathsf{sd}(\hat{N}) \tag{14}$$

and the standard deviation of the abundance-at-age estimate for age a is

$$\sigma_a = \mathsf{sd}(\hat{N}_a). \tag{15}$$

A common summary of the uncertainty of the estimate of the total number $\hat{N}$ is the coefficient of variation,

$$\mathsf{cv}_{\text{total}} = \frac{\sigma_{\text{total}}}{\hat{N}}. \tag{16}$$

To have a summary over all ages, we define

$$\sigma_{\text{age}} = \sqrt{\sum_a \sigma_a^2}. \tag{17}$$

By independence, $\sigma_{\text{age}} = \sigma_{\text{total}}$, but (17) is still a useful measure without the independence assumption.

We have identified five sources to the total uncertainty:

- Three correction factors (Section 3.2). The parameters in each of these are uncertain.
- Spatial-temporal uncertainty (Section 3.7). The acoustic measurements cover only a small part of the area. Furthermore, since the fish are moving around, measurements at the same location, but at different times, are in general unequal.

- Age/length uncertainty (Section 3.6). The lengths and ages are measured for only a small amount of the fish, and on few locations.

These five sources are independent, since they are based on different and independent data. We decompose the total variance σ^2_{total} into the contribution from each source separately. The contribution from the ith uncertainty source is calculated as

$$\frac{\hat{\sigma}^2_{\text{total}} - \hat{\sigma}^2_{\text{total}}(i)}{\sum_{i=1}^{5} \hat{\sigma}^2_{\text{total}} - \hat{\sigma}^2_{\text{total}}(i)}, \tag{18}$$

where $\hat{\sigma}^2_{\text{total}}(i)$ is computed without uncertainty source i. The decomposition (18) enable comparisons of the relative contributions to the uncertainty in abundance-at-age and total abundance.

3.4 Quantifying the total uncertainty by simulation

The estimates (based on the improved estimator described in Section 3.2) are not model based, and we therefore suggest to quantify their uncertainties by the following resampling method:

1. Let θ denote all the parameters in the three correction Equations (9), (10) and (11). Simulate a set of parameters θ^* by sampling from their estimated uncertainty distributions (Section 3.5).

2. Draw a bootstrap sample of age/length data, taking into account the inhomogeneity between trawl hauls (Section 3.6). Calculate the average of the squared bootstrapped length $\overline{l^2}^*$ and the estimated proportion-at-age $\hat{p}^*_a$.

3. For each acoustic signal measurement i, estimate the corresponding density of fish $\hat{\rho}^*_i$ by (12) and (13), conditioned on the simulated parameters and the bootstrapped length data.

4. Draw a bootstrap sample $\hat{\rho}^{**}_i, i = 1, \ldots, n$, of fish densities from the densities $\hat{\rho}^*_i, i = 1, \ldots, n$, calculated above, (partly) taking into account correlations in space and time. Calculate the average $\bar{\rho}^{**}$ (Section 3.7).

5. Calculate the corresponding estimates $\hat{N}^{**}$ of total abundance by Equation (6) and $\hat{N}^{**}_a$ of abundance-at-age by Equation (8).

6. Repeat the procedure above B=1 000 times, and calculate standard deviations from the bootstrap distributions of the total abundance and the abundance-at-age.

This procedure is performed per sub-area (squares in Vesteraalen and three fjords in the Vestfjord system), and the uncertainty over a whole area is found by combining the sub-area estimates assuming independence between sub-areas. Assuming independence between sub-areas is the standard estimation practice and is suggested by Rivoirard et al. (2000). This approximation holds better the larger the sub-areas are.

3.5 Parameter simulation

The parameters in the correction formulas are drawn from their estimated distributions as described below.

1. **Vessel avoidance:** The parameter c_d in Equation (9) can be written as $c_d = c \cdot \exp(a_d)$, where c is a constant, adjusting for bias due to log scale modelling. c is estimated without uncertainty, so we ignore its uncertainty here. The remaining parameters $(\boldsymbol{a}, b)$ and their variance-covariance matrix Σ, where $\boldsymbol{a}$ is the vector of all a_d's are estimated. The parameter estimates are asymptotically normally distributed. Hence, to sample the parameters with uncertainty, we sample from the multivariate normal distribution $N\left((\widehat{\boldsymbol{a}, b}), \widehat{\Sigma}\right)$.

2. **Shadowing effect:** Foote (1999) estimates λ in Equation (10) with standard error. As above, to sample the parameter with uncertainty, we sample from the normal distribution $N\left(\hat{\lambda}, \widehat{\mathsf{Var}}(\hat{\lambda})\right)$.

3. **Depth dependent target strength:** Ona (2003) estimates the parameters σ_0 and γ in Equation (11). The standard errors and correlation between the two parameter estimates are represented by a set of pairwise bootstrap replicates. To sample the parameters with uncertainty, we sample from the bootstrap replicates.

3.6 Age/length uncertainty

The bootstrap of the trawl samples has to take into account the inhomogeneity between trawl hauls. First, M trawl hauls are drawn with replacements from the M real trawl hauls. Assume that in trawl haul m, $m = 1, 2, \ldots, M$, there are

$n_m^{\mathsf{age\ read}}$ samples for which age is read,

$n_m^{\mathsf{non\text{-}readable\ age}}$ samples for which age is impossible to read and

$n_m^{\mathsf{length\ only}}$ samples for which age is not read, but length is measured.

The total number of fish for trawl haul m is

$$n_m = n_m^{\mathsf{age\ read}} + n_m^{\mathsf{non\text{-}readable\ age}} + n_m^{\mathsf{length\ only}}.$$

Within each bootstrap haul m^*, $n_{m^*}^{\mathsf{age\ read}}$ fish (age/length pairs) are drawn with replacement among the $n_m^{\mathsf{age\ read}}$ real samples. $n_{m^*}^{\mathsf{non\text{-}readable\ age}}$ fish are drawn with replacement among the $n_m^{\mathsf{non\text{-}readable\ age}}$ real samples. Finally, $n_{m^*}^{\mathsf{length\ only}}$ fish lengths are drawn with replacement among all the n_m real samples.

3.7 Quantifying spatial-temporal uncertainty by block bootstrap

To simplify the description of the assessment of the spatial-temporal uncertainty, assume first that we have observed the true densities $\rho_i, i = 1, \ldots, n$, instead of their estimates $\hat{\rho}_i$. The spatial-temporal uncertainty is due to the fact that the true fish density ρ over an area is estimated by a sample mean $\bar{\rho}$ in Equation (6).

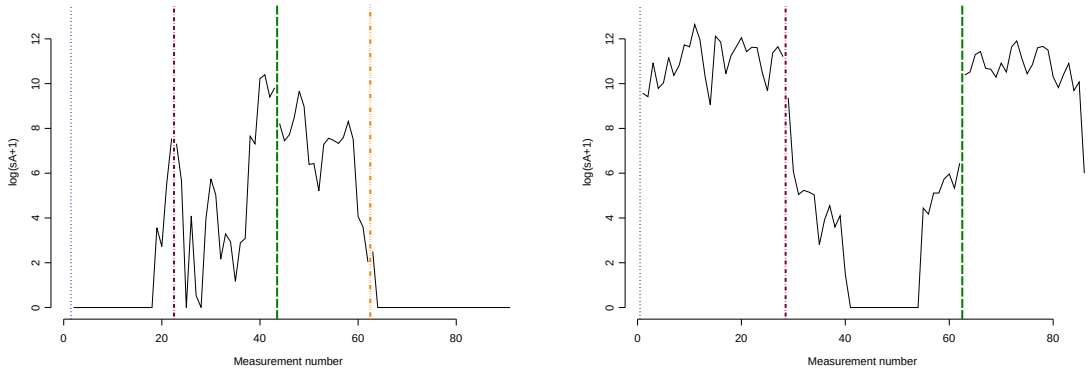

Figure 4: Example of data series ($\log(s_A + 1)$) with stratum limits. On the left, the measurements are along the survey line from between the two X's in the overview of the 2004 Vesteraalen survey in Figure 2. On the right, the measurements are along the survey line to the east of the X (Ofotfjord) in the overview of the 2004 Vestfjord system survey.

Ordinary bootstrapping of ρ_i, based on independent random sampling with replacement, would ignore the spatial-temporal correlations and under-estimate the uncertainty. On the other hand, it is complex to take this uncertainty fully into account. Note that since the fish are moving around, measurements at the same location, but at different times, will in general be different. The observed densities ρ_i vary both in the two-dimensional space and in time, but we will regard it as a time series, using the time dimension only. Since the locations are ordered along transects, using the time dimension alone still take into account some of the spatial relations. To sample from the distribution of the sample mean of a time series, we use the block bootstrap (Carlstein, 1986; Künsch, 1989).

The block bootstrap requires that the time series is stationary. Therefore, we first divide the time series into non-overlapping strata, with approximate stationarity within strata. Each strata has at least 20 measurements (20 nmi). In the Vesteraalen area, the stratum limits are chosen automatically, with a new stratum each time the survey line moves into a new sub-area or square in Figure 2. This is illustrated in the left panel of Figure 4, which shows the logarithm of the acoustic measurements from a part of the 2004 survey. The stationary assumptions (constant mean and variance) within strata holds approximately, since each stratum is relatively small. In the Vestfjord system, where the pattern of transect lines is more complex, we select the stratum limits manually based on a visual inspection. This is illustrated in the right panel of Figure 4 which displays the logarithm of acoustic measurements from the sub-area Ofotfjord in the Vestfjord system 2004.

Within each stratum, we perform block bootstrap. Block bootstrap consists of dividing the time series into blocks of consecutive observations, and then sampling (with replacement) a suitable number of blocks from the collection of all possible blocks. The correlation structure is preserved within each block, but not between blocks. If the block lengths are large enough, the break between blocks will become less important. We have used block length 5 (nmi). We use overlapping blocks, and to avoid undesired edge effects, the data are wrapped around a circle and form additional blocks, called circular bootstrap (Lahiri, 2003).

The true densities ρ_i are not observed, but the corresponding $\hat{\rho}_i^*$ in stage 3 of Section 3.4 acts as such, conditioned on the simulated parameters from stage 1 and the bootstrapped length data from stage 2. Therefore, in stage 4, the bootstrap sample $\hat{\rho}_i^{**}, i = 1, \ldots, n$, are drawn from $\hat{\rho}_i^*$ by the circular block bootstrap.

A major advantage of this approach is its simplicity. The many zero measurements pose no problems, as long as the time series is stationary within each stratum and our choice of block length is appropriate. Furthermore, there is no need for data transformation. The drawback is of course the simplification that the two spatial dimensions and the time dimension is handled by the time dimension alone. Furthermore, the stationary assumption holds better in some sub-areas than in others. In the right column in Figure 4, the assumptions hold rather well on the left and the right, but not in the middle. The assumption of independence between sub-areas holds better with longer strata, but longer strata lead to less stationarity.

4 Results

4.1 Effect of bias corrections

Area and year	No correction	Shadow correction	Shadow correction and depth dependent TS	Vessel avoidance, shadow correction and depth dependent TS
Vestfjord system 2001	14.2	17.2	7.5	14.3
Vestfjord system 2002	5.9	7.1	3.3	3.6
Vestfjord system 2003	5.0	5.7	2.6	3.4
Vesteraalen 2003	28.0	30.0	11.7	54.7
Total 2003	**33.0**	**35.7**	**14.3**	**58.1**
Vestfjord system 2004	3.3	3.7	1.7	2.5
Vesteraalen 2004	21.3	21.9	8.7	46.4
Total 2004	**24.6**	**25.6**	**10.4**	**48.9**

Table 2: Estimated number of herring (10^9), from Equation (6), 2001–2004.

N is estimated using Equation (6) and the corrections in Section 3.2. To investigate the effect of the signal corrections, we have included the estimate of N without any correction, with shadow correction, with the cumulative effect of shadowing and depth dependent target strength and the cumulative effect of vessel avoidance, shadowing and depth dependent target strength (in that order). Table 2 summarises the results. As expected, the shadow correction

adjusts the estimates upwards, the depth dependent target strength adjusts the estimates downwards and vessel avoidance adjusts the estimates upwards. The cumulative effect is sometimes positive (the Vestfjord system 2001, Vesteraalen 2003 and 2004) and sometimes negative (the Vestfjord system 2002, 2003 and 2004). The adjustment upwards is particularly apparent in Vesteraalen. The depth distribution of fish can explain this.

In Figure 5, we have shown the cumulative effects of the corrections per depth. (Note that the axes are not equal.) Large parts of the stock in Vesteraalen were distributed between 0 and 100 m, and the effect of the vessel avoidance formula (9) is particularly strong in these depth layers. For the Vestfjord system the same year, however, there are some fish in the upper layers, but the majority are situated from 200 m and downwards.

Area and year	Cv
Vestfjord system 2001	16.5 %
Vestfjord system 2002	18.0%
Vestfjord system 2003	18.5%
Vesteraalen 2003	20.0%
Total 2003	**19.0 %**
Vestfjord system 2004	19.5%
Vesteraalen 2004	33.0%
Total 2004	**31.5 %**

Table 3: Estimated coefficient of variation (cv) for total abundance N, from Equation (16), 2001–2004.

4.2 Total uncertainty for abundance and abundance-at-age

The various surveys are summarised in Table 3, showing the estimated coefficients of variation (cv) for total abundance for each survey. The estimated cv is quite stable at 16.5–20%, except for Vesteraalen 2004 with a cv of 33%. The high cv in 2004 is mostly due to the patchiness of the acoustic data, with very high and zero measurements close by. Of the 21 sub-areas with non-zero measurements (see Figure 2), two sub-areas contain about 2/3 of the total number of fish, and most of the variance. In 2003, the acoustic data were more equally spread (not shown here), which gives a lower spatial-temporal uncertainty. Another reason for the high cv in 2004 is that there are more fish in the upper layers, with more corresponding uncertainty due to the vessel avoidance correction.

4.3 Decomposition of uncertainty contribution

Table 4 shows the contribution of each uncertainty source to the total uncertainty, calculated by Equation (18). A graphical summary is given in the upper part of Figure 6. Generally, the contribution of uncertainty from shadowing is small (0–3%), and relatively largest when the shadowing effect is highest (Table 2). The contribution from depth dependent target strength is higher (1.5–12.5%), and its contribution is particularly low when most of the fish are distributed in the upper depth layers. The uncertainty due to uncertain vessel avoidance parameters is high (16.5–41%). The uncertainty due to age/length is quite small, but not negligible, with 4% in Vesteraalen 2004, stemming from the large heterogeneities in the length

distributions between trawl hauls that year. Finally, the spatial-temporal uncertainty is the largest contributor (46–78%).

Similarly, the age-specific uncertainty $\hat{\sigma}_{\text{age}}$ can be decomposed into the contribution from each source as in Table 5 and the lower part of Figure 6. The general picture is the same as for N, but the age/length uncertainty is now more dominant (17–52.5%), and its relative contribution is comparable with the spatial-temporal component. However, if we focus on one particular age, the uncertainty may be higher or lower. Comparing Vesteraalen 2003 and 2004, the uncertainty contributions from age and length are 17% and 46%, respectively. This is due to the large heterogeneities between trawl hauls in Vesteraalen 2004, while the heterogeneities between trawl hauls in Vesteraalen 2003 were particularly low (not shown here).

5 Discussion

This study has demonstrated the combined effect of correcting for vessel avoidance, shadowing and depth dependent target strength on the estimate of the abundance of Norwegian spring-spawning herring. Applied on data from the November/December survey from 2001–2004, we have demonstrated the potential dramatic effect of the corrections. Furthermore, we have demonstrated how the total uncertainty is affected by uncertainty in the parameters of vessel avoidance, shadowing and depth dependent target strength and uncertainty from trawl hauls and spatial-temporal coverage. Note that we have not included modelling error for the acoustic signal corrections. There is reason to believe that the formula for vessel avoidance is not fully developed. For instance, the vessel avoidance experiments we utilised are all conducted during two days in Tysfjord in the Vestfjord system. In a more recent experiment in Ofotfjord (2004), the observed avoidance was much smaller than in (Vabø et al., 2002). Vessel avoidance experiments out in Vesteraalen, with possibly higher background noise from waves, might also give different results.

The approach taken here may be enhanced in various ways. In addition to the vessel avoidance, modelling of the spatial-temporal uncertainty is an area for further research. We assume stationarity within strata and independence between strata. These assumptions are not always satisfied in practice and the consequences thereof are unclear. The large number of zeros, combined with extreme observations and the concurrent sampling in time and space is challenging to model. An answer might be a space-time model. In that case, the naive plug-in estimate is replaced by an integral over time and space.

The possible errors in age reading can be taken into account if the distribution of true age given observed age is known. In that case, this can be built into the model by an extra layer in the bootstrap sampling of age.

After correcting for vessel avoidance, shadowing and depth dependent target strength, there might still be considerable bias, for instance diurnal variability. In addition, the largest contributor by far to bias, is to not cover the whole distribution are of the fish. This happened (at least) in 2002, where almost the entire survey was conducted in the Vestfjord system, while herring were reported in Vesteraalen. In addition, migration during the survey might induce a bias, and the migration (or the bias?) is difficult to estimate and model.

However, the main framework is believed to be a promising tool for focusing the effort for reducing the uncertainty in the abundance estimates. The present results imply that the focus should be on vessel avoidance and spatial-temporal sampling if the total abundance is

most important. If abundance-at-age is equally important, more trawl hauls should be done, at least if there are large heterogeneities between trawl hauls. How many trawl hauls which are needed is also an area of further research.

Acknowledgements

This research was funded by the Institute of Marine Research and the Research Council of Norway, research grant no. 143249/140.

References

Carlstein, E. (1986). The use of subseries methods for estimating the variance of a general statistic from a stationary sequence. *The Annals of Statistics*, 14:1171–1179.

Foote, K. (1987). Fish target strengths for use in echo integrator surveys. *Journal of the Acoustic Society of America*, 82:981–987.

Foote, K. (1999). Extinction cross-section of norwegian spring-spawning herring. *ICES Journal of Marine Science*, 56:606–612.

Künsch, H. R. (1989). The jacknife and the bootstrap for general stationary observations. *The Annals of Statistics*, 17:1217–1261.

Lahiri, S. (2003). *Resampling Methods for Dependent Data*. Springer.

Ona, E. (2003). An expanded target-strength relationship for herring. *ICES Journal of Marine Science*, 60:493–499.

Rivoirard, J., Simmons, J., Foote, K., Fernandez, P., and Bez, N. (2000). *Geostatistics for Estimating Fish Abundance*. Blackwell Science.

Thoresen, R., Gjøsæter, H., and de Barros, P. (1998). The acoustic method as used in the abundance estimation of capelin (Mallotus villosus Müller) and herring (Clupea harengus Linne) in the Barents Sea. *Fisheries Research*, pages 27–37.

Vabø, R., Olsen, K., and Huse, I. (2002). The effect of vessel avoidance of wintering Norwegian spring spawning herring. *Fisheries Research*, 58:59–77.

Zhao, X. and Ona, E. (2003). Estimation and compensation models for the shadowing effect in dense fish aggregations. *ICES Journal of Marine Science*, 60:155–163.

Area and year	Total uncertainty	Shadow correction	Depth dependent TS correction	Vessel avoidance correction	Age/length	Spatial-temporal
Vestfjord system 2001	100%	0.0%	12.5%	31.5%	2.0%	54.0%
Vestfjord system 2002	100%	3.0%	8.0%	28.0%	1.5%	59.5%
Vestfjord system 2003	100%	1.0%	11.0%	41.0%	1.0%	46.0%
Vesteraalen 2003	100%	0.0%	5.0%	16.5%	0.5%	78.0%
Vestfjord system 2004	100%	0.0%	8.0%	28.5%	0.0%	63.5%
Vesteraalen 2004	100%	0.0%	1.5%	21.0%	4.0%	73.5%

Table 4: Relative contribution to uncertainty of total abundance.

Area and year	Total uncertainty	Shadow correction	Depth dependent TS correction	Vessel avoidance correction	Age/length	Spatial-temporal
Vestfjord system 2001	100%	0.0%	6.5%	17.0%	52.5%	24.0%
Vestfjord system 2002	100%	1.0%	4.0%	17.5%	45.5%	32.0%
Vestfjord system 2003	100%	0.5%	8.0%	30.5%	28.5%	32.5%
Vesteraalen 2003	100%	0.0%	4.0%	14.0%	17.0 %	65.0%
Vestfjord system 2004	100%	0.0%	5.5%	22.0%	27.5%	45.0%
Vesteraalen 2004	100%	0.0%	1.0%	13.0%	46.0%	40.0%

Table 5: Relative contribution to uncertainty of abundance-at-age.

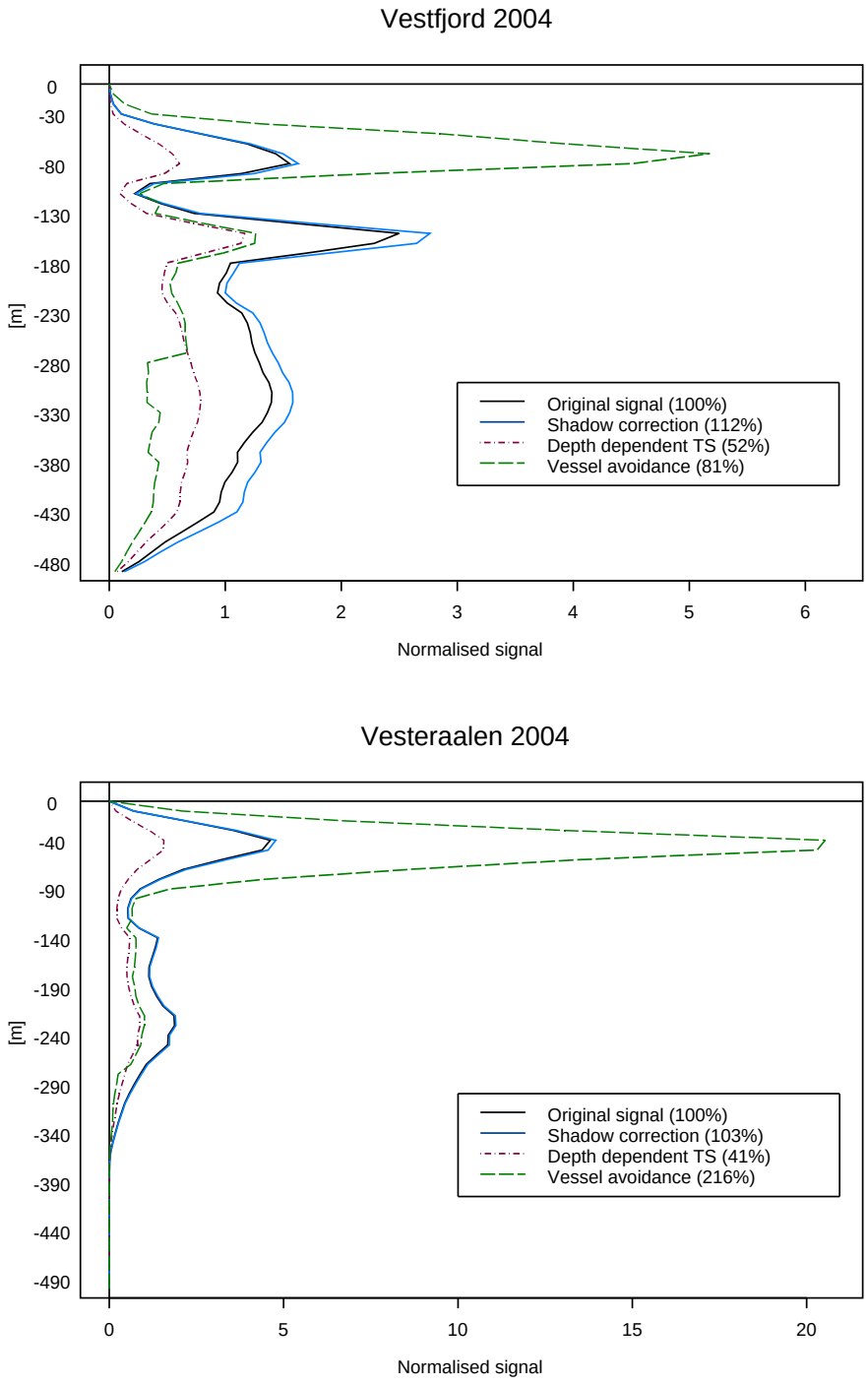

Figure 5: The cumulative effect of corrections, relative to the original, uncorrected signal,the Vestfjord system (upper) and Vesteraalen (lower) 2004. The original signal is normalised to 100% in average over the water column. The numbers in parenthesis are total cumulative effects.

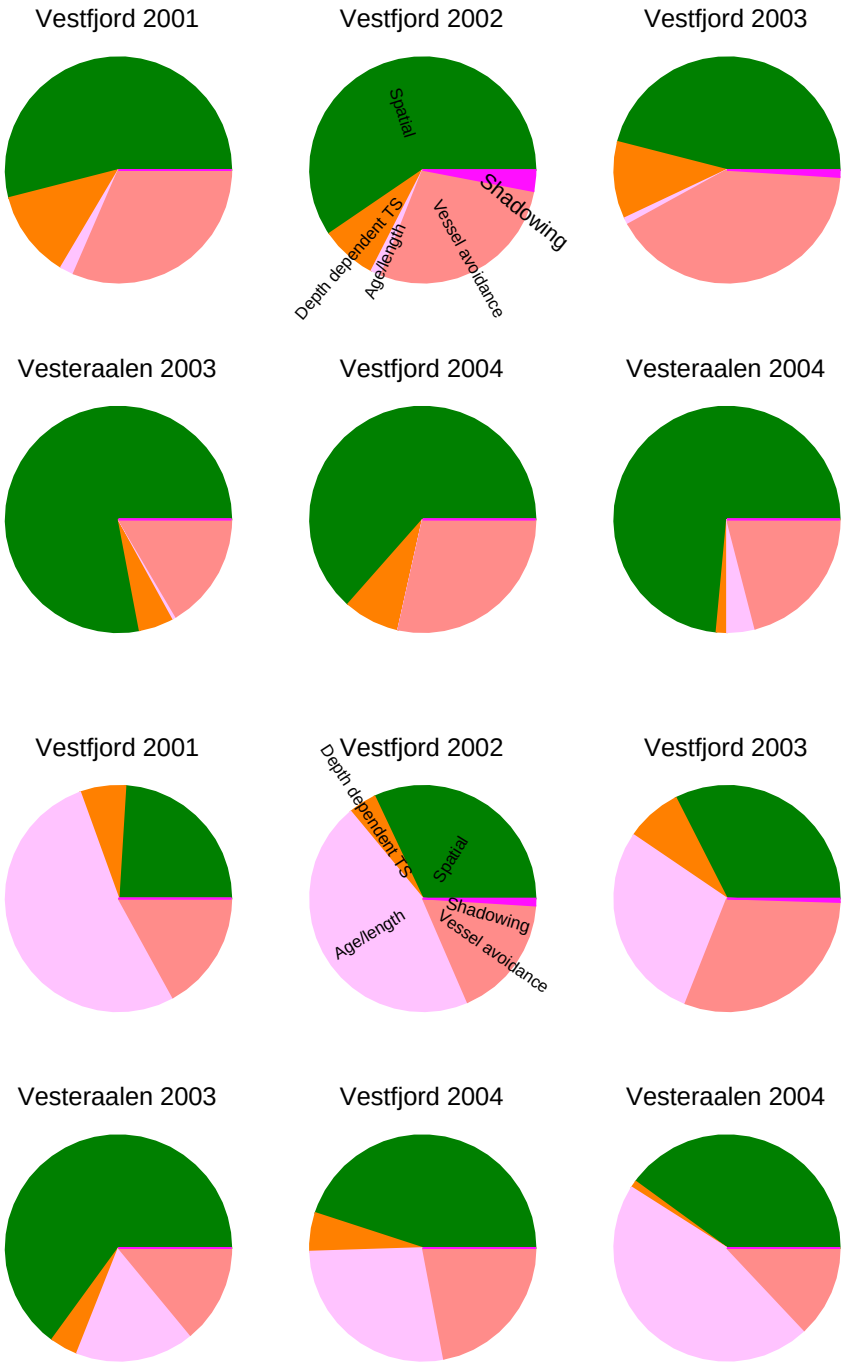

Figure 6: Relative contribution to uncertainty of total abundance (upper six), and abundance-at-age (lower six), as given in Table 4 and 5.